

1 Is within-host viral community assembly shaped by local adaptation?

2

3 Maija Jokinen<sup>1</sup>, Hanna Susi<sup>1,2</sup> & Anna-Liisa Laine<sup>1</sup>

4 <sup>1</sup> Organismal and Evolutionary Biology Research Programme, Faculty of Biological and  
5 Environmental Sciences, PO BOX 65, 00014, University of Helsinki, Finland

6 <sup>2</sup> Department of Agricultural Sciences, Faculty of Agriculture and Forestry, PO BOX 27,  
7 00014, University of Helsinki, Finland

8

9 Corresponding author: Maija Jokinen [maija.jokinen@helsinki.fi](mailto:maija.jokinen@helsinki.fi)

10 Running title: Viral local adaptation

11 local adaptation, coevolution, viruses, host-parasite coevolution

12

13

14

15

16

17

18 Abstract

19 Host-parasite coevolution describes the continuous reciprocal selection driving host defense  
20 and parasite infectivity, with direct consequences for disease dynamics. While abundant  
21 evidence exists for coevolution shaping host-parasite dynamics within the ‘one host-one  
22 parasite’ framework, hosts are typically infected by multiple parasites and the extent to which  
23 coevolutionary processes shape within-host parasite communities remains poorly understood.  
24 Investigating these interactions is essential for understanding how coevolution drives parasite  
25 diversity, competition, and coexistence within hosts. Here, we conducted a local adaptation  
26 experiment to investigate the effects of coevolution on within-host viral community assembly  
27 in *Plantago lanceolata*. Greenhouse-grown individuals were reciprocally transplanted into  
28 wild populations during natural viral epidemics. We combined small-RNA sequencing to  
29 identify the viral communities and joint species distribution modelling to quantify the effects  
30 of local adaptation, population and host characteristics on viral community assembly. Our  
31 results show that host populations vary in the extent to which local adaptation influences  
32 within-host viral diversity. Across all populations, host maternal line and origin population  
33 were the main determinants of viral community composition and infection status. The effects  
34 varied across virus families, suggesting virus-specific assembly processes and variation in the  
35 potential for coevolution to shape these interactions.

36  
37

38

39

40

41

42 Introduction

43 Coevolutionary theory predicts reciprocal selection to drive key interaction traits in hosts and  
44 parasites – resistance and infectivity, respectively (1,2). Coevolution is fundamental for  
45 understanding host-parasite interactions and disease dynamics in nature, as the presence of  
46 parasites depends on the availability of susceptible hosts. Indeed, host-parasite interactions  
47 provide some of the most compelling evidence for the theory of coevolution, often  
48 demonstrated through local adaptation experiments (3–6). However, much of this work has  
49 focused on the one-host-one-parasite framework, although in nature hosts are rarely infected  
50 by a single parasite and often support complex parasite communities (7–10). Despite the  
51 growing interest in within-host parasite communities in natural environments, there remains a  
52 gap in our understanding of how coevolution can shape these complex communities (11,12).

53 Genetic variation and genotype-genotype specificity in the interaction are prerequisites  
54 for coevolution. Indeed, the ability to infect or resist infection can be genotype-dependent:  
55 some parasite genotypes can infect only certain host genotypes, while some host genotypes  
56 exhibit resistance to specific parasite genotypes (13–15). This variation is maintained by  
57 evolutionary mechanisms, such as parasite-imposed negative frequency-dependent selection  
58 and arms-race dynamics, which can favour different host genotypes in different populations,  
59 contributing to local adaptation (3,15,16). Notably, the outcome of host genotype  $\times$  parasite  
60 genotype interactions may be altered under multiple parasite attack (17,18), with co-occurring  
61 parasites influencing community assembly either directly through parasite-parasite interactions  
62 (19,20) or indirectly through host-mediated responses (14,21). If host colonization ability – a  
63 trait expected to be shaped by coevolution – is sensitive to co-occurring parasites, then we may  
64 expect community assembly to be shaped by both ecological and evolutionary dynamics (22).  
65 The community monopolization hypothesis – evoked to explain evolutionary priority effects  
66 – predicts that locally adapted resident species can have a competitive advantage over later

67 arriving individuals, potentially influencing parasite community dynamics (23,24). It has been  
68 demonstrated that adaptation can reduce competitive dominance with direct consequences for  
69 community assembly (24), and that locally adapted parasites can influence the composition of  
70 the entire community (25,26).

71 Viruses, similar to other parasites, can form highly diverse communities (20,27–32).  
72 As obligate parasites, viral reproduction relies on the virus' ability to infect and hijack host cell  
73 machinery (33), making host-virus interactions a key factor in shaping viral communities  
74 (14,34,35). Here, to investigate how viral community assembly is influenced by coevolution,  
75 we conducted a reciprocal transplant experiment, by placing naïve *Plantago lanceolata*  
76 individuals as sentinels in sympatric and allopatric populations during naturally occurring viral  
77 epidemics. We sampled the plant individuals at the end of the growth season for small-RNA  
78 sequencing to characterize viral communities and used joint species distribution modelling (36)  
79 to tease apart the effects of local adaptation, population and host characteristics on viral  
80 community assembly. Specifically, we ask: i) Can we detect viral local adaptation? ii) What is  
81 the importance of local adaptation in determining viral community assembly? iii) What is the  
82 role of population and host characteristics in viral community assembly?

83

84 Materials and Methods

85 Study species

86 The host, *Plantago lanceolata*, is a perennial herb reproducing clonally with side rosettes or  
87 sexually with wind-dispersed pollen (37). *Plantago lanceolata* occurs worldwide, and in  
88 Finland, *P. lanceolata* can be found mainly in SW Finland. In the Åland Islands (an area  
89 spanning 50 × 70 km), *P. lanceolata* forms a large network consisting of over 4000 small  
90 fragmented populations (38).

91        The *P. lanceolata* host populations in the Åland Islands harbour complex viral  
92    communities (19,20). Five novel *P. lanceolata* infecting viruses have been characterised from  
93    this system, and PCR primers have been developed for their detection (14,39,40). Viral  
94    symptoms in wild hosts are challenging to identify but can include yellowing or redness of the  
95    leaf, curliness and necrotic lesions (40–42). *Plantago lanceolata latent virus* (PILV) infection  
96    has been linked to yellowing of the leaf (40,43).

97

98    Preparation of host plant material and field experiment

99    To investigate the role of local adaptation in viral community assembly, we conducted a  
100   reciprocal transplant experiment in three *P. lanceolata* populations (ID: s: 9205, 876, and 950)  
101   in the Åland Islands. In autumn 2020, seeds were collected from eight individuals per studied  
102   population and germinated in early April 2021 with the aim of obtaining up to 15 offspring per  
103   maternal line. The seeds from 24 maternal lines (Supplementary table 1), were sown in peat  
104   pots with a 3:1 mixture of potting soil and sand and then placed in a growth chamber with a  
105   16:8 h light-dark cycle. After three weeks, the seedlings were transferred to the greenhouse and  
106   replanted into 10 cm ×10 cm pots filled with a 1:1 mixture of potting soil and sand. The plants  
107   were watered as needed and, when large enough, fertilized weekly with NPK fertilizer (7:2:2).  
108   During the growth period in the greenhouse, leaf samples were collected for PCR screening to  
109   confirm that each maternal line was virus-free of PILV, *Plantago latent caulimovirus*, *Plantago*  
110   *betapartitivirus*, *Plantago enamovirus*, and *Plantago closterovirus*, all of which are among the  
111   most common viruses in the Åland Islands populations (39,40). Two weeks prior to the  
112   transplant experiment, the plants were treated with fungicide (Bordeaux mixture).

113        In early June 2021, the greenhouse-grown naïve plants were taken to the Åland Islands  
114   and placed in their transplant populations. For each maternal line, five offspring were placed

115 in their sympatric *P. lanceolata* population and five in each of the two allopatric populations  
116 (Figure 1). For four maternal lines with fewer offspring, priority was given to sympatric  
117 placement, and the remaining individuals were distributed among the two allopatric  
118 populations (Supplementary table 1). Finally, the experiment consisted of 348 plants across the  
119 three transplant populations (Supplementary table 1). The plants were randomly placed among  
120 the natural vegetation and kept in pots placed inside plastic boxes (approximately 13 cm × 11  
121 cm) to isolate them from the local soil. To minimize within-population spatial effects, we  
122 shuffled the plants among the plastic boxes three times per week for the duration of the  
123 experiment. The plants were watered as needed.

124 After six weeks of exposure, a 3 cm<sup>2</sup> piece of leaf tissue was collected for RNA  
125 extraction and snap-frozen in liquid nitrogen. At this time, we also recorded host characteristics  
126 that prior work suggests could affect viral infections on *P. lanceolata*. Plant size was measured  
127 as  $n \times A$ , where  $n$  is the number of leaves and  $A = \pi ab$ , where  $a$  is the half axis of the width of  
128 the largest leaf, and  $b$  is the half axis of the length of the largest leaf (14,19).

129

130 RNA extraction and RNA purification

131 Total RNA was extracted using a modified acid phenol-chloroform extraction protocol (44). A  
132 3 cm<sup>2</sup> leaf tissue sample was ground in liquid nitrogen, after which 800 µl of warm extraction  
133 buffer was added and mixed thoroughly. The extraction buffer consisted of 2%  
134 hexadecyltrimethylammonium bromide (Sigma-Aldrich USA), 2% of polyvinylpyrrolidone K-  
135 30 (MW 40 000, Sigma-Aldrich USA), 100 mM of Tris-HCl (pH 8.0, Thermo Fisher Scientific,  
136 USA), 25 mM of Ethylenediaminetetraacetic acid (pH 8.9, Sigma-Aldrich, USA), 2.0 M of  
137 NaCl (Sigma-Aldrich, USA) and 2% of β-mercaptoethanol (Sigma-Aldrich, USA). Next, 800  
138 µl of acid phenol-chloroform-isoamyl alcohol (IAA; 25:24:1) was added, and the sample was

139 centrifuged at 13500 rpm for 15 minutes at RT. The supernatant was transferred to a clean tube,  
140 mixed with 1 ml phenol-chloroform-IAA and centrifuged under the same conditions. RNA was  
141 precipitated by adding 160  $\mu$ l of 10 M LiCl and incubating overnight at +4 °C. The following  
142 day, samples were purified with chloroform-IAA (24:1) purification step and washed twice  
143 with ethanol. The RNA pellet was resuspended in 25  $\mu$ l of nuclease-free water and treated with  
144 Ambion® DNA-free™ DNA removal Kit (Invitrogen, USA). RNA concentration was  
145 measured using Nanodrop 2000 (Thermo Fischer Scientific, USA) and Qubit (Thermo Fischer  
146 Scientific, USA), and RNA was stored at -80 °C.

147

148 Small-RNA sequencing and bioinformatic pipeline  
149 To identify the viral communities present in the sentinel plants, we assigned the samples to  
150 small-RNA (sRNA) sequencing. From the 348 sampled experimental plants, we randomly  
151 selected samples from three individuals from each maternal line from each transplant  
152 population to be assigned for sRNA sequencing. From maternal line 876-4, we sequenced three  
153 samples from the sympatric transplant population but only one sample from one of the  
154 allopatric populations, resulting in 211 samples assigned for sRNA sequencing. The RNA  
155 extracted from the selected samples was diluted with nuclease-free water and sent to the  
156 sequencing facility according to the sequencing company's instructions (Fasteris SA,  
157 Switzerland).

158 The sRNA sequencing and library preparation were carried out at Fasteris SA  
159 (Switzerland). Small-RNA cDNA libraries were prepared using QIAseq miRNA Library Kit  
160 (Qiagen) according to Fasteris SA Small RNA-Seq Gel-free protocol with 100 ng of total RNA.  
161 Sequencing was performed using Illumina NovaSeq 6000 (Illumina Inc, San Diego, California,  
162 USA) and targeted insert sizes from 0 nt to 43 nt with an average library yield of 1779 Mb.

163 Inserts with sizes from 20 nt to 25 nt were selected for bioinformatic analyses. Sequencing  
164 adapter removal was done using Trimmomatics software (45), and the reads were de novo  
165 assembled to contigs using VirusDetect software (46). VirusDetect software conducts  
166 BLASTX and BLASTN searches against curated plant virus database (vrl\_Plants\_248\_U100)  
167 of VirusDetect for each sample separately. We used default parameters BLASTX and  
168 BLASTN searches, default similarity 25 % and p-value 1e-5. We then assigned the obtained  
169 contigs to virus family level for the statistical analyses (Supplementary table 2).

170

171 Statistical analysis

172 All statistical analyses were conducted in R (version 4.2.2; (47). To test whether local  
173 adaptation influenced host infection status (infected by any studied virus= 1, not infected by  
174 any studied virus = 0), we fitted generalized linear mixed models (GLMM) using the  
175 "glmmTMB" R-package (48) with binomial distribution and logit link function. Specifically,  
176 we constructed GLMMs to test the two key metrics of local adaptation: i) local *vs.* foreign and  
177 ii) home *vs.* away (49,50). For the local *vs.* foreign model (LF), a categorical variable  
178 representing sympatry or allopatry, nested within transplant population, was included as a fixed  
179 effect. Seed origin population and plant size were included as additional fixed effects and  
180 maternal line nested within seed origin population was included as a random effect to account  
181 for genetic variation among hosts. For the home *vs.* away model (HA), the model structure was  
182 identical, except that the categorical variable of sympatry or allopatry was nested within seed  
183 origin population and included as a fixed effect. Model assumptions were assessed using R-  
184 package "DHARMA" (51). The significance of the main effects were evaluated using Wald X<sup>2</sup>  
185 tests (function "Anova" in R-package "car"; (52). For significant effects, pairwise comparisons  
186 of the estimated marginal means were performed using functions "contrasts" and "emmeans"

187 from the R-package “emmeans” (version 1.8.8; (53), applying Tukey’s method for multiple  
188 comparisons.

189 To investigate the effects of local adaptation, population and host characteristics on  
190 within-host viral diversity, while also accounting for viral (co-)occurrence patterns in the  
191 transplant experiment, we implemented Joint Species Distribution Modelling (JSDM) using  
192 the hierarchical modelling of species communities (HMSC) framework (54,55). HMSC is a  
193 hierarchical generalized linear mixed model with Bayesian inference and allows the analysis  
194 of multiple species’ responses to ecological variables while incorporating species- and  
195 community-level parameters and accounting for covariation among species. The response  
196 variables in our HMSC model were the occurrences of the three most prevalent virus families:  
197 *Caulimoviridae*, *Partitiviridae* and *Pospivirodae*. As fixed effect predictors, we included 1)  
198 maternal line ID, 2) seed origin population, 3) sympatry/allopattery, 4) plant size, and 5) signs  
199 of herbivory. Transplant population was included as a random effect. Including  
200 sympatry/allopattery as a fixed effect allowed us to directly estimate the effect of local adaptation  
201 in our model. We used four separate Markov chain Monte Carlo (MCMC) chains to sample the  
202 posterior distribution. Each chain was run for 1 875 000 iterations, and the first 625 000 were  
203 discarded as burn-in. Subsequently, the remaining iterations were thinned by 5000, resulting in  
204 250 posterior samples per chain. Finally, we obtained a total of 1000 posterior samples across  
205 all four chains. The model fit was evaluated by examining explanatory and predictive  
206 performance via ten-fold cross-validation, using Tjur’s coefficient of determination (Tjur  $R^2$ )  
207 and area under the curve (AUC), respectively. The HMSC analyses were ran using the R-  
208 package “Hmsc” (version 3.0-14).

209

210

211 Results

212 Description of the sRNA sequencing data

213 From the 211 sequenced individuals, the sRNA sequencing yielded on average 23,799,485  
214 reads per plant tissue sample (min 17,364,260; max 49,152,805; SD 7,738,962). The  
215 VirusDetect pipeline assembled 2374 contigs ranging from 41 to 2080 nt in length (mean length  
216 of 159 nt and SD 163 nt). Of these, 11% of contigs had virus-specific BLASTN hits with 80–  
217 100% identity (mean 93%), while 89% had BLASTX hits with 22–100% identity (mean 67%).

218 In total, we assembled 1151 plant virus-associated contigs across the 211 individuals,  
219 representing six plant virus families: *Tymoviridae*, *Botourmiaviridae*, *Closteroviridae*,  
220 *Partitiviridae*, *Caulimoviridae* and *Pospiviroidae* (Figure 2C, Supplementary table 2). From  
221 each family, we identified 1 to 3 virus genera and 3 to 842 contigs for each genus. At the species  
222 level, we acquired BLAST hits to 1 to 15 species, depending on the virus genus (Supplementary  
223 table 2). Overall, 26% of the host individuals were infected, and of those 86% were colonized  
224 by one virus family and 14% by two virus families. The most prevalent families were  
225 *Caulimoviridae* and *Pospiviroidae* (both in 43% of the infected individuals), whereas  
226 *Tymoviridae* and *Botourmiaviridae* were the rarest (both in 2% of the infected individuals;  
227 Figure 2C).

228

229 Analysis of viral local adaptation: local vs. foreign

230 Using the local vs. foreign criterion, we observed indications of viral local adaptation in  
231 transplant population 876, where local hosts had higher infection rates than foreign hosts. A  
232 similar trend was observed in population 950, where local hosts showed the second-highest  
233 infection rates (Figure 2A). Conversely, in population 9205, local hosts harboured fewer  
234 infections than foreign hosts – suggesting viral maladaptation. However, the GLMM (LF) did

235 not provide statistical support for these trends (Wald  $X^2 = 1.53$ ,  $P = 0.673$ ; Table 1). Seed  
236 origin populations differed significantly in infection rates (Wald  $X^2 = 7.37$ ,  $P = 0.025$ ; Table  
237 1), with individuals originating from population 9205 having significantly fewer infections  
238 than those originating from population 876 (Figure 2A, Supplementary table 3A; estimate =  
239 2.071, SE = 0.778, z-ratio = 2.661,  $P = 0.021$ ).

240 Analysis of viral local adaptation: home vs. away

241 Applying the home vs. away criterion, we found no evidence of viral local adaptation (Figure  
242 2B). Hosts from populations 876 and 950 had lower infection rates in their respective home  
243 populations than in their away populations, suggesting viral maladaptation (Figure 2B). Our  
244 statistical analysis (model HA) did not detect significant differences in infection rates between  
245 home and away habitats. However, model coefficients for the “sympatry” term nested within  
246 seed origin population were lower, suggesting higher infection rates in away habitats  
247 (Supplementary table 4). Additionally, seed origin population significantly influenced host  
248 infection status (Wald  $X^2 = 9.09$ ,  $P=0.010$ ; Table 2). Post hoc comparisons showed that  
249 individuals from population 876 had significantly higher infection rates than those from  
250 population 9205 (estimate = 1.818, SE = 0.649, z-ratio = 2.802,  $P = 0.014$ ; Supplementary table  
251 3B., Figure 2B and C).

252 Analysis of viral (co-)occurrence patterns

253 We applied the HMSC approach to investigate the factors influencing the (co-)occurrence of  
254 the detected virus families in a local adaptation experiment. The model predicted virus family  
255 occurrences well, although model performance varied among virus families (Supplementary  
256 table 5). Tjur  $R^2$  and AUC were used to quantify the explanatory and predictive performance  
257 of the model, with a mean Tjur  $R^2$  of 0.27 (range among the detected virus families 0.10-0.47)  
258 and a mean AUC of 0.89 (0.80-0.98). The predictive power of the model was based on ten-fold

259 cross-validations, where the mean Tjur  $R^2$  was 0.19 (range 0.01 - 0.4) and the mean AUC was  
260 0.74 (range 0.54-0.88; Supplementary table 5) varying among virus families.

261 In terms of contributions to the explained variation in our HMSC model, host maternal  
262 line was the strongest determinant of viral occurrences, explaining on average 62% of the  
263 variance. However, the effect varied among virus families and was most pronounced for  
264 *Pospiviroidae* (73%) and less important in explaining *Partitiviridae* (60%) and *Caulimoviridae*  
265 (54%) occurrences (Figure 3, Supplementary table 6). For example, maternal line 876-6,  
266 displayed the highest infection rates, with 89% of the individuals infected (Figure 2C). Seed  
267 origin population was the second most important predictor, explaining on average of 29% of  
268 the variance. The effect of host maternal line varied among virus families, with a more  
269 pronounced role for *Caulimoviridae* (35%) and *Partitiviridae* (33%), while being less  
270 important for explaining the occurrences of *Pospiviroidae* (18%; Figure 3, Supplementary table  
271 6). Consistent with this, individuals from seed origin population 876 harboured 50% of all  
272 detected viral infections, whereas individuals originating from population 9205 harboured only  
273 16% of all infections (Figure 2C).

274 Host plant size accounted for an average of 4% of the variation in viral occurrences,  
275 with the strongest effect observed for *Caulimoviridae* (7%). Local adaptation  
276 (sympatry/allopatry) had a smaller role in contributing to explained variation, accounting for  
277 2% on average across virus families (Figure 3, Supplementary table 6). Herbivory had minimal  
278 effect, explaining only 0% to 0.1% of the viral occurrences. The random effect of transplant  
279 population explained on average 2% of the variation across virus families and was slightly  
280 more important in explaining *Pospiviroidae* occurrences (4%, Figure 3, Supplementary table  
281 6). Residual correlations among virus families at the random level were not significant,  
282 suggesting that after accounting for the effects of the fixed explanatory variables, viral  
283 occurrences were not influenced by interactions between virus families.

284 Discussion

285 Here, we used a reciprocal transplant experiment combined with sRNA sequencing and JSDM  
286 modelling to investigate the role of local adaptation in shaping within-host viral (co-  
287 )occurrences. Although we observed trends suggesting viral local adaptation and maladaptation  
288 when applying the local *vs.* foreign and home *vs.* away criteria, the effects were not statistically  
289 significant. Instead, we found host maternal line and host seed origin population to be the most  
290 important determinants of host infection status and viral community structure. The strength of  
291 these effects varied across virus families, indicating virus-specific assembly processes and  
292 variation in the extent to which coevolution shapes these interactions. Jointly our results  
293 identify key drivers of viral community assembly and provide insight into how within-host  
294 dynamics could scale up to predict the ecological and evolutionary consequences of disease in  
295 natural systems.

296 Using sRNA sequencing, we detected viruses from six virus families, five of which  
297 have been previously identified from this system (20,43). Overall, 21% of the sampled sentinel  
298 plants were infected, exhibiting a lower infection rate than previously reported from hosts in  
299 this system (20,43). Despite the low overall infection prevalence, we found individuals  
300 originating from population 876 harbouring significantly higher infection rates than those from  
301 population 9205. Viral community composition also varied among seed origin populations and  
302 among maternal lines. Individuals from seed origin population 876 harboured viruses from five  
303 different virus families (*Caulimoviridae*, *Pospiviroidae*, *Partitiviridae*, *Botourmiaviridae* and  
304 *Closteroviridae*), whereas individuals from population 950 were infected by only three virus  
305 families (*Pospiviroidae*, *Caulimoviridae* and *Partitiviridae*). The overall lower infection  
306 prevalence may be due to differences in exposure time to viral epidemics and additionally, viral  
307 prevalence may vary annually due to several factors, such as temperature, humidity and vector

308 behaviour — components of natural systems that are difficult to control in a field experiment  
309 (56–58).

310 Using a reciprocal transplant experimental approach, we were able to apply the two key  
311 metrics of local adaptation: local *vs.* foreign and home *vs.* away. While we observed signs of  
312 viral local adaptation in transplant population 876 under the local *vs.* away criterion, the pattern  
313 was not statistically significant (GLMM LF). Similarly, analysis on the home *vs.* away metric  
314 showed no statistically significant effect of local adaptation on host infection status (GLMM  
315 HA). In line with these results, when investigating the effects of local adaptation on viral (co-  
316 )occurrence patterns with JSDM in the HMSC framework, we found local adaptation to explain  
317 on average only 2.3% of the viral occurrences. However, when using the home *vs.* away  
318 criterion (GLMM HA), individuals from seed origin populations 876 and 950 harboured the  
319 lowest infection rates in their home populations, suggesting viral maladaptation. Patterns of  
320 maladaptation are not unexpected given the dynamic, cyclic nature of coevolutionary  
321 interactions between the host and its parasite (59). In the Åland Islands *P. lanceolata*  
322 populations are highly fragmented, and the connectivity levels of the populations vary (60,61)  
323 and consequently too high or low gene flow between populations could facilitate parasite  
324 maladaptation (59,62–64). Previous studies have shown that well-connected host populations  
325 are less affected by disease (65,66), a phenomenon that is likely due to higher resistance  
326 diversity in these populations maintained by gene flow (61).

327 Seed origin population was a strong predictor of host infection status. Individuals  
328 originating from population 876 were more frequently infected and harboured the most diverse  
329 viral communities. In contrast, hosts from population 9205 exhibited high resistance to viral  
330 infection and consequently harboured less complex viral communities. Our HMSC analysis  
331 mirrored these findings, identifying maternal line and seed origin population as the strongest  
332 determinants of viral occurrence across virus families, explaining on average 62% and 29% of

333 the variation, respectively (Figure 3). The variation in infection rates among host origin  
334 populations, together with the strong maternal line effects for viral occurrences across virus  
335 families, highlights host genetic diversity as a key driver of viral community assembly and  
336 composition in this system. Although evidence for viral local adaptation was limited, the  
337 variation in infections prevalence among host maternal lines indicates strong potential for  
338 coevolution, as genetic variation is a main driver of coevolution (67–69). Moreover, high host  
339 genetic diversity in natural populations can mitigate disease risk, a phenomenon known as the  
340 monoculture effect (70,71).

341 Hosts encounter a myriad of parasites throughout their lives (43,72–74), and these  
342 interactions can have far-reaching consequences for host-parasite coevolution and population  
343 dynamics (75). Despite this, much of the research on local adaptation has focused on pairwise  
344 host-parasite interactions (76–78), with little focus on the role of parasite communities in  
345 coevolutionary processes. To our knowledge, our study is among the first to study viral local  
346 adaptation within a community ecology framework. After accounting for host attributes, we  
347 found no evidence of virus-virus interactions shaping within-host viral diversity. Instead, host  
348 characteristics, represented by maternal line and host seed origin population, emerged as the  
349 most important predictor of viral community structure and host infection status. Our findings  
350 highlight the importance of host genetic variation in shaping viral communities and contribute  
351 to the growing field of viral community ecology research. Understanding the drivers of  
352 complex host-parasite interactions and processes at the community level is essential for  
353 predicting how disease dynamics scale up from individuals to populations and understanding  
354 the ecological and evolutionary conditions from which novel viral diseases may emerge.

355

356

357 Acknowledgements

358 We thank Krista Raveala, Aura Palonen, Suvi Sallinen, Marijke Iso-Kokkila and Jere Lentonen  
359 for the help with the transplant experiment and RNA extractions. We thank Suvi Sallinen for  
360 the help with statistical analysis. The CSC – IT Center for Science, Finland, is acknowledged  
361 for computational resources. The work was funded by grants from the European Research  
362 Council (AdG 101097545 Co-EvoChange), and Academy of Finland (334276, 362242) to A.-  
363 L.L. and Academy of Finland (321441) to H.S.

364 Author contributions

365 M.J., H.S. and A.-L.L. designed the study. M.J. performed the field experiment, data collection,  
366 and statistical analysis. M.J., H.S. and A-L.L. prepared the manuscript.

367 Conflict of Interest

368 The authors declare no conflict of interests.

369 Data availability Statement

370 The data and R scripts used in this study have been submitted to GitHub  
371 (<https://github.com/maiabajoki/ViRAL21>).

372

373 References

- 374 1. Buckingham LJ, Ashby B. Coevolutionary theory of hosts and parasites. *J Evol Biol.*  
375 2022;35(2):205–24.
- 376 2. Thompson JN, Cunningham BM. Geographic structure and dynamics of coevolutionary  
377 selection. *Nature.* 2002;417(6890):735–8.

378 3. Decaestecker E, Gaba S, Raeymaekers JAM, Stoks R, Kerckhoven LV, Ebert D, et al.  
379 Host-parasite ‘Red Queen’ dynamics archived in pond sediment. *Nature*.  
380 2007;450(7171):870–3.

381 4. Greischar MA, Koskella B. A synthesis of experimental work on parasite local adaptation.  
382 *Ecol Lett*. 2007;10(5):418–34.

383 5. Kaltz O, Shykoff JA. Local adaptation in host–parasite systems. *Hered* 1998 814. 1998 Oct  
384 1;81(4):361–70.

385 6. Dybdahl MF, Storfer A. Parasite local adaptation: Red Queen versus Suicide King. *Trends*  
386 *Ecol Evol*. 2003 Oct 1;18(10):523–30.

387 7. Johnson PTJ, Hoverman JT. Parasite diversity and coinfection determine pathogen  
388 infection success and host fitness. *Proc Natl Acad Sci U S A*. 2012 June 5;109(23):9006–  
389 11.

390 8. Ben-Ami F, Mouton L, Ebert D. The effects of multiple infections on the expression and  
391 evolution of virulence in a *Daphnia*-endoparasite system. *Evolution*. 2008;62(7):1700–11.

392 9. Tollenaere C, Susi H, Nokso-Koivisto J, Koskinen P, Tack A, Auvinen P, et al. SNP Design  
393 from 454 Sequencing of *Podosphaera plantaginis* Transcriptome Reveals a Genetically  
394 Diverse Pathogen Metapopulation with High Levels of Mixed-Genotype Infection. *PLoS*  
395 ONE. 2012 Dec 27;7(12).

396 10. Griffiths EC, Pedersen AB, Fenton A, Petchey OL. The nature and consequences of  
397 coinfection in humans. *J Infect*. 2011 Sept;63(3):200–6.

398 11. Betts A, Gray C, Zelek M, MacLean RC, King KC. High parasite diversity accelerates host  
399 adaptation and diversification. *Science*. 2018;360(6391):907–11.

400 12. Hall AR, Ashby B, Bascompte J, King KC. Measuring Coevolutionary Dynamics in  
401 Species-Rich Communities. *Trends Ecol Evol*. 2020 June 1;35(6):539–50.

402 13. Hily JM, Poulicard N, Mora MÁ, Pagán I, García-Arenal F. Environment and host  
403 genotype determine the outcome of a plant–virus interaction: from antagonism to  
404 mutualism. *New Phytol*. 2016 Jan 1;209(2):812–22.

405 14. Sallinen S, Norberg A, Susi H, Laine AL. Intraspecific host variation plays a key role in  
406 virus community assembly. *Nat Commun*. 2020;11(1):1–11.

407 15. Gandon S. Local adaptation and the geometry of host-parasite coevolution. *Ecol Lett*.  
408 2002;5(2):246–56.

409 16. Woolhouse MEJ, Webster JP, Domingo E, Charlesworth B, Levin BR. Biological and  
410 biomedical implications of the co-evolution of pathogens and their hosts. *Nat Genet*.  
411 2002;32(4):569–77.

412 17. Tollenaere C, Susi H, Laine AL. Evolutionary and Epidemiological Implications of  
413 Multiple Infection in Plants. *Trends Plant Sci*. 2016 Jan 1;21(1):80–90.

414 18. Karvonen A, Fenton A, Sundberg LR. Sequential infection can decrease virulence in a  
415 fish–bacterium–fluke interaction: Implications for aquaculture disease management. *Evol  
416 Appl.* 2019 Dec 1;12(10):1900–11.

417 19. Jokinen M, Sallinen S, Jones MM, Sirén J, Guilbault E, Susi H, et al. The first arriving  
418 virus shapes within-host viral diversity during natural epidemics. *Proc R Soc B* [Internet].  
419 2023 Sept 13 [cited 2023 Nov 30];290(2006). Available from:  
420 <https://royalsocietypublishing.org/doi/10.1098/rspb.2023.1486>

421 20. Norberg A, Susi H, Sallinen S, Baran P, Clark NJ, Laine AL. Direct and indirect viral  
422 associations predict coexistence in wild plant virus communities. *Curr Biol.* 2023 May  
423 8;33(9):1665–1676.e4.

424 21. Tollenaere C, Susi H, Laine AL. Evolutionary and Epidemiological Implications of  
425 Multiple Infection in Plants. *Trends Plant Sci.* 2016 Jan 1;21(1):80–90.

426 22. Gorter FA, Manhart M, Ackermann M. Understanding the evolution of interspecies  
427 interactions in microbial communities. *Philos Trans R Soc B* [Internet]. 2020 May 11 [cited  
428 2024 Oct 14];375(1798). Available from:  
429 <https://royalsocietypublishing.org/doi/10.1098/rstb.2019.0256>

430 23. Urban MC, De Meester L. Community monopolization: local adaptation enhances priority  
431 effects in an evolving metacommunity. *Proc R Soc B Biol Sci.* 2009 Dec  
432 7;276(1676):4129–38.

433 24. Nadeau CP, Farkas TE, Makkay AM, Papke RT, Urban MC. Adaptation reduces  
434 competitive dominance and alters community assembly. *Proc R Soc B* [Internet]. 2021 Feb  
435 24 [cited 2023 Apr 14];288(1945). Available from:  
436 <https://royalsocietypublishing.org/doi/10.1098/rspb.2020.3133>

437 25. Pantel JH, Duvivier C, Meester LD. Rapid local adaptation mediates zooplankton  
438 community assembly in experimental mesocosms. *Ecol Lett.* 2015;18(10):992–1000.

439 26. Gómez P, Paterson S, De Meester L, Liu X, Lenzi L, Sharma MD, et al. Local adaptation  
440 of a bacterium is as important as its presence in structuring a natural microbial community.  
441 *Nat Commun* [Internet]. 2016 [cited 2024 Oct 11]; Available from:  
442 [www.nature.com/naturecommunications](http://www.nature.com/naturecommunications)

443 27. Breitbart M, Hewson I, Felts B, Mahaffy JM, Nulton J, Salamon P, et al. Metagenomic  
444 analyses of an uncultured viral community from human feces. *J Bacteriol.* 2003  
445 Oct;185(20):6220–3.

446 28. Brum JR, Ignacio-espinoza JC, Roux S, Doulcier G, Acinas SG, Alberti A, et al. Ocean  
447 Viral Communities. *Science.* 2015;348(6237):1261411–98.

448 29. Durham DM, Sieradzki ET, Ter Horst AM, Santos-Medellín C, Winston C, Bess A, et al. Substantial  
449 differences in soil viral community composition within and among four  
450 Northern California habitats. *ISME Commun* 2022 21. 2022 Oct 13;2(1):1–5.

451 30. Pratama AA, van Elsas JD. The ‘Neglected’ Soil Virome – Potential Role and Impact.  
452 *Trends Microbiol.* 2018;26(8):649–62.

453 31. Rwanhni MA, Daubert S, Úrbez-Torres JR, Cordero F, Rowhani A. Deep sequencing  
454 evidence from single grapevine plants reveals a virome dominated by mycoviruses. *Arch  
455 Virol.* 2011;156(3):397–403.

456 32. Yang K, Wang X, Hou R, Lu C, Fan Z, Li J, et al. Rhizosphere phage communities drive  
457 soil suppressiveness to bacterial wilt disease. *Microbiome.* 2023;11(1):1–18.

458 33. Christiaansen A, Varga SM, Spencer JV. Viral manipulation of the host immune response.  
459 *Curr Opin Immunol.* 2015;36:54.

460 34. Coloma S, Gaedke U, Sivonen K, Hiltunen T. Frequency of virus-resistant hosts determines  
461 experimental community dynamics. *Ecology.* 2019;100(1):1–10.

462 35. Roossinck MJ, Bazán ER. Symbiosis: Viruses as Intimate Partners. *Annu Rev Virol.* 2017  
463 Sept 29;4:123–39.

464 36. Norberg A, Abrego N, Blanchet FG, Adler FR, Anderson BJ, Anttila J, et al. A  
465 comprehensive evaluation of predictive performance of 33 species distribution models at  
466 species and community levels. *Ecol Monogr.* 2019 Aug 1;89(3):e01370.

467 37. Sagar GR, Harper JL. *Plantago Major* L., *P. Media* L. and *P. Lanceolata* L. *J Ecol.* 1964  
468 Mar;52(1):189.

469 38. Ojanen SP, Nieminen M, Meyke E, Pöyry J, Hanski I. Long-term metapopulation study of  
470 the Glanville fritillary butterfly (*Melitaea cinxia*): Survey methods, data management, and  
471 long-term population trends. *Ecol Evol.* 2013 Oct 1;3(11):3713–37.

472 39. Susi H, Laine AL, Filloux D, Krabberger S, Farkas K, Bernardo P, et al. Genome sequences  
473 of a capulavirus infecting *Plantago lanceolata* in the Åland archipelago of Finland. *Arch  
474 Virol.* 2017 July 1;162(7):2041–5.

475 40. Susi H, Filloux D, Frilander MJ, Roumagnac P, Laine A liisa. Diverse and variable virus  
476 communities in wild plant populations revealed by metagenomic tools. 2019;

477 41. Adams IP, Skelton A, Macarthur R, Hodges T, Hinds H, Flint L, et al. Carrot yellow leaf  
478 virus is associated with carrot internal necrosis. *PLoS ONE.* 2014 Nov 3;9(11).

479 42. Biswas KK, Bhattacharyya UK, Palchoudhury S, Balram N, Kumar A, Arora R, et al. Dominance of recombinant cotton leaf curl Multan-Rajasthan virus associated with cotton  
480 leaf curl disease outbreak in northwest India. *PLOS ONE.* 2020 Apr 1;15(4):e0231886.

482 43. Susi H, Filloux D, Frilander MJ, Roumagnac P, Laine AL. Diverse and variable virus  
483 communities in wild plant populations revealed by metagenomic tools. *PeerJ* [Internet].  
484 2019 [cited 2020 Feb 19];2019(1). Available from: <http://doi.org/10.7717/peerj.6140>

485 44. Chang S, Puryear J, Cairney J. A simple and efficient method for isolating RNA from pine  
486 trees. *Plant Mol Biol Report.* 1993;11(2):113–6.

487 45. Bolger AM, Lohse M, Usadel B. Genome analysis Trimmomatic: a flexible trimmer for  
488 Illumina sequence data. 2014;30(15):2114–20.

489 46. Zheng Y, Gao S, Padmanabhan C, Li R, Galvez M, Gutierrez D, et al. VirusDetect: An  
490 automated pipeline for efficient virus discovery using deep sequencing of small RNAs.  
491 *Virology*. 2017 Jan 1;500:130–8.

492 47. R Foundation for Statistical, Computing, Vienna A. R: A language and environment for  
493 statistical computing. 2022; Available from: <https://www.r-project.org/>

494 48. Brooks ME, Kristensen K, Van Benthem KJ, Magnusson A, Berg CW, Nielsen A, et al.  
495 glmmTMB Balances Speed and Flexibility Among Packages for Zero-inflated Generalized  
496 Linear Mixed Modeling. *R J*. 2017;9:2.

497 49. Kawecki TJ, Ebert D. Conceptual issues in local adaptation. *Ecol Lett*. 2004 Dec  
498 1;7(12):1225–41.

499 50. Blanquart F, Kaltz O, Nuismer SL, Gandon S. A practical guide to measuring local  
500 adaptation. *Ecol Lett*. 2013 Sept;16(9):1195–205.

501 51. Hartig F. DHARMA: Residual Diagnostics for Hierarchical (Multi-Level / Mixed)  
502 Regression Models. 2022; Available from: <https://cran.r-project.org/package=DHARMA>

503 52. Fox J, Weisberg S. An R Companion to Applied Regression. Sage Publ. 2019;

504 53. Russell V, Lenth RV, BB [ctb], PB [ctb], IGV [ctb], MH [ctb], MJ [ctb], JL [ctb], FM [ctb],  
505 JP [ctb], HR [ctb], SH. Package “Emmeans”. 2018;

506 54. Ovaskainen O, Tikhonov G, Norberg A, Guillaume Blanchet F, Duan L, Dunson D, et al.  
507 How to make more out of community data? A conceptual framework and its  
508 implementation as models and software. *Ecol Lett*. 2017 May 1;20(5):561–76.

509 55. Ovaskainen O, Abrego N. Joint Species Distribution Modelling [Internet]. Cambridge  
510 University Press; 2020 [cited 2022 Oct 17]. Available from:  
511 <https://www.cambridge.org/core/product/identifier/9781108591720/type/book>

512 56. Trebicki P. Climate change and plant virus epidemiology. *Virus Res*.  
513 2020;286(June):198059.

514 57. Kendig AE, Borer ET, Mitchell CE, Power AG, Seabloom EW. Characteristics and drivers  
515 of plant virus community spatial patterns in US west coast grasslands. *Oikos*. 2017 Sept  
516 1;126(9):1281–90.

517 58. Jeger MJ, Fereres A, Malmstrom CE, Mauck KE, Wintermantel WM. Epidemiology and  
518 Management of Plant Viruses Under a Changing Climate. *Phytopathology*. 2023 Nov  
519 4;113(9):1620–1.

520 59. Kaltz O, Gandon S, Michalakis Y, Shykoff JA. Local maladaptation in the anther-smut  
521 fungus *Microbotryum violaceum* to its host plant *Silene latifolia*: Evidence from a cross-  
522 inoculation experiment. *Evolution*. 1999;53(2):395–407.

523 60. Jousimo J, Tack AJM, Ovaskainen O, Mononen T, Susi H, Tollenaere C, et al. Ecological  
524 and evolutionary effects of fragmentation on infectious disease dynamics. *Science*.  
525 2014;344(6189):1289–93.

526 61. Höckerstedt L, Siren JP, Laine AL. Effect of spatial connectivity on host resistance in a  
527 highly fragmented natural pathosystem. *J Evol Biol.* 2018;31(6):844–52.

528 62. Gandon S. Local adaptation and the geometry of host-parasite coevolution. *Ecol Lett.*  
529 2002;5(2):246–56.

530 63. Hoeksema JD, Forde SE. A meta-analysis of factors affecting local adaptation between  
531 interacting species. *Am Nat.* 2008 Mar;171(3):275–90.

532 64. Oppliger A, Vernet R, Baezà M. Parasite local maladaptation in the Canarian lizard  
533 *Gallotia galloti* (Reptilia: Lacertidae) parasitized by haemogregarine blood parasite. *J Evol*  
534 *Biol.* 1999;12(5):951–5.

535 65. Höckerstedt L, Numminen E, Ashby B, Boots M, Norberg A, Laine AL. Spatially  
536 structured eco-evolutionary dynamics in a host-pathogen interaction render isolated  
537 populations vulnerable to disease. *Nat Commun.* 2022;13(1):1–11.

538 66. Carlsson-Granér U, Thrall PH. Host resistance and pathogen infectivity in host populations  
539 with varying connectivity. *Evolution.* 2015 Apr 1;69(4):926–38.

540 67. Paterson S, Vogwill T, Buckling A, Benmayor R, Spiers AJ, Thomson NR, et al. Antagonistic  
541 coevolution accelerates molecular evolution. *Nature.* 2010 Mar 11;464(7286):275–8.

543 68. Buckingham LJ, Ashby B. Coevolutionary theory of hosts and parasites. *J Evol Biol.* 2022  
544 Feb 1;35(2):205–24.

545 69. Laine AL, Burdon JJ, Dodds PN, Thrall PH. Spatial variation in disease resistance: From  
546 molecules to metapopulations. *J Ecol.* 2011;99(1):96–112.

547 70. Laine AL, Burdon JJ, Dodds PN, Thrall PH. Spatial variation in disease resistance: From  
548 molecules to metapopulations. *J Ecol.* 2011 Jan;99(1):96–112.

549 71. Ridenhour BJ, Nuismer SL. Polygenic traits and parasite local adaptation. *Evolution.*  
550 2007;61(2):368–76.

551 72. Vayssier-Taussat M, Kazimirova M, Hubalek Z, Hornok S, Farkas R, Cosson JF, et al. Emerging horizons for tick-borne pathogens: From the ‘one pathogen-one disease’ vision  
552 to the pathobiome paradigm. *Future Microbiol.* 2015 Dec 1;10(12):2033–43.

554 73. Susi H, Barrès B, Vale PF, Laine AL. Co-infection alters population dynamics of infectious  
555 disease. *Nat Commun.* 2015 Jan 8;6(1):1–8.

556 74. Boots M, White A, Best A, Bowers R. The importance of who infects whom: The evolution  
557 of diversity in host resistance to infectious disease. *Ecol Lett.* 2012;15(10):1104–11.

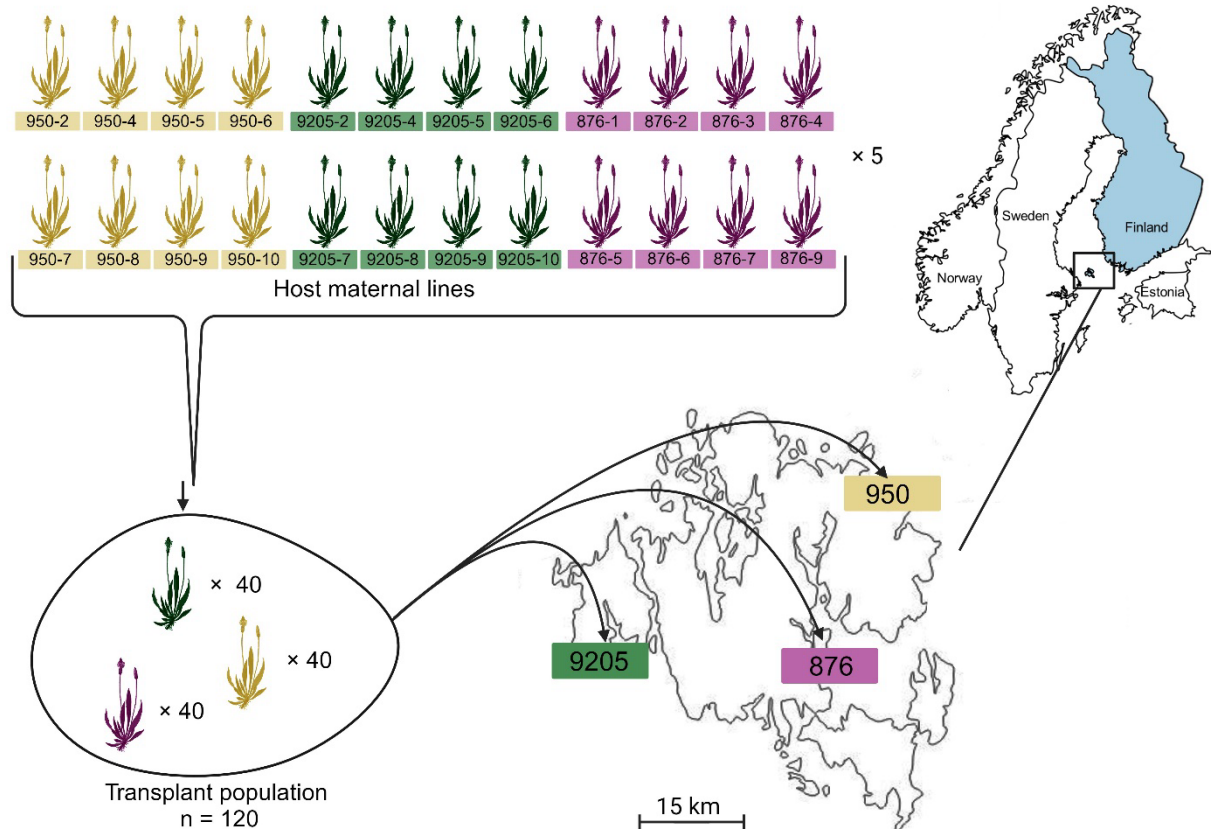
558 75. Hall AR, Ashby B, Bascompte J, King KC. Measuring Coevolutionary Dynamics in  
559 Species-Rich Communities. *Trends Ecol Evol.* 2020;35(6):539–50.

560 76. Ridenhour BJ, Nuismer SL. Polygenic traits and parasite local adaptation. *Evolution.* 2007  
561 Feb;61(2):368–76.

562 77. Laine AL. Detecting local adaptation in a natural plant-pathogen metapopulation: A  
563 laboratory vs. field transplant approach. *J Evol Biol.* 2007 Sept;20(5):1665–73.

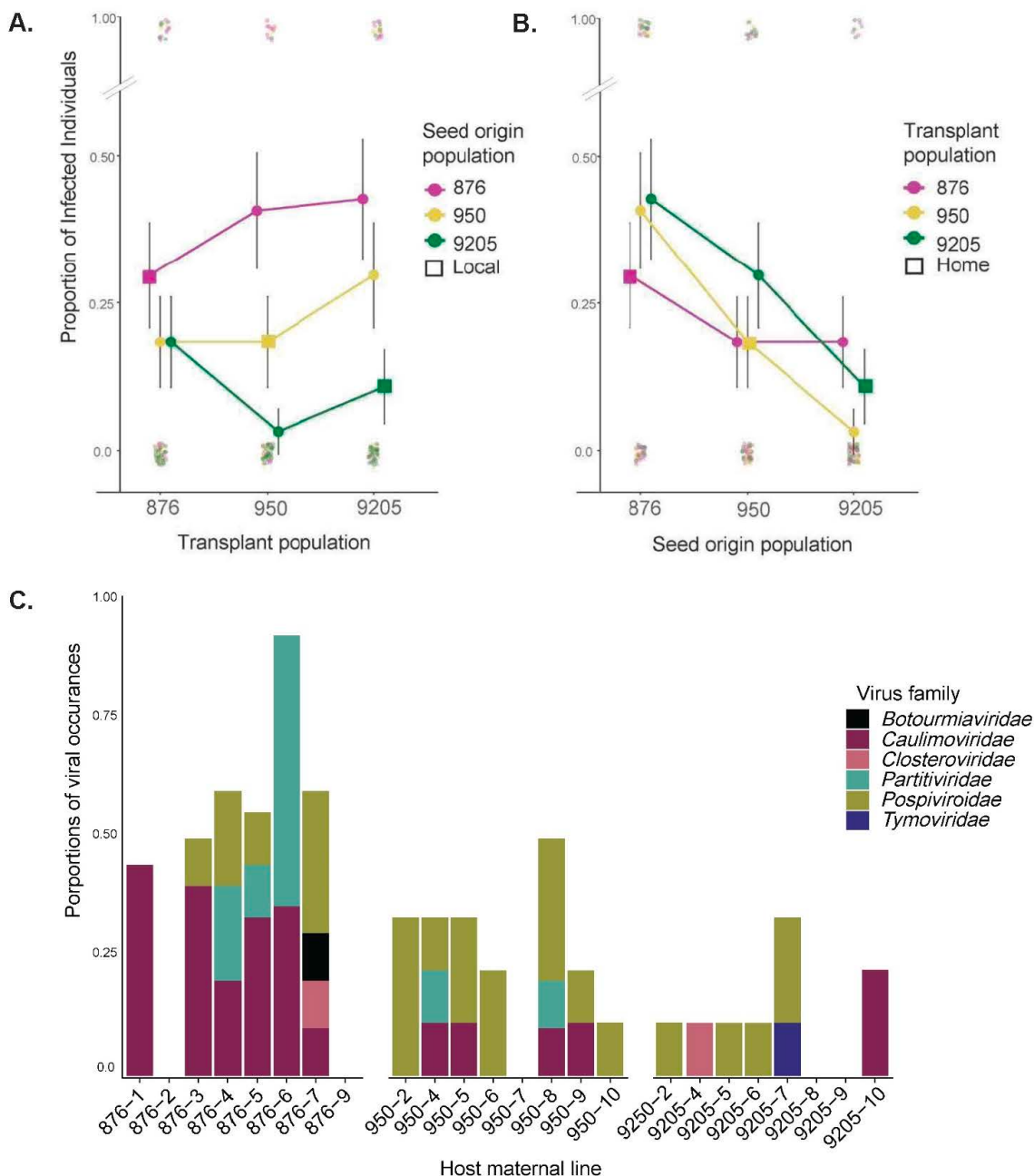
564 78. Mauck KE, De Moraes CM, Mescher MC. Evidence of Local Adaptation in Plant Virus  
565 Effects on Host–Vector Interactions. *Integr Comp Biol.* 2014 July 1;54(2):193–209.

566



567

568 Figure 1. Reciprocal transplant experiment where *Plantago lanceolata* individuals from 24  
569 maternal lines originating from three populations were transplanted into their sympatric and  
570 two allopatric populations during natural viral epidemics. We placed 40 individuals into  
571 sympatric population and ~80 individuals into two allopatric populations, with a total of 348  
572 plant individuals across three populations in the Åland Islands SW Finland.



573

574 Figure 2. Proportions of virus infected *Plantago lanceolata* host individuals in a reciprocal  
575 transplant experiment using (A) local vs. foreign, (B) home vs. away metrics of local  
576 adaptation, and (C) infection pattern across host maternal (n = 24) line grouped by seed origin  
577 population. In panel A, colours indicate the seed origin populations and the squares mark the  
578 local host. In panel B, the colours represent the transplant populations and the squares mark  
579 the home habitat of the host (purple = seed origin/transplant population 876, yellow = seed  
580 origin/transplant population 950, and green = seed origin/transplant population 9205). In panel  
581 C colours represent the six virus families detected with sRNA sequencing.

582

583

584

585 Table 1. Type II Wald  $\chi^2$  test for Generalized linear mixed model estimating the effects of plant  
 586 size, seed origin population, transplant population and local vs. foreign metric of local  
 587 adaptation on host infection status (1=infected, 0=uninfected) in a reciprocal transplant  
 588 experiment in the Åland Islands (model LF).

589

Fixed effect	<i>Wald <math>\chi^2</math></i>	Df	<i>p</i> -value
Plant size	1.71	1	0.190
<b>Seed origin population</b>	<b>7.37</b>	<b>2</b>	<b>0.025</b>
Transplant population	1.99	2	0.369
Transplant population : sympatry/allopatry	1.53	3	0.673

590

591

592 Table 2. Type II Wald  $\chi^2$  test for Generalized linear mixed model testing for the effects of plant  
 593 size, seed origin population, transplant population and home vs. away metric of local adaptation  
 594 on host infection status (1=infected, 0=uninfected) in a reciprocal transplant experiment in the  
 595 Åland Islands (model HA).

596

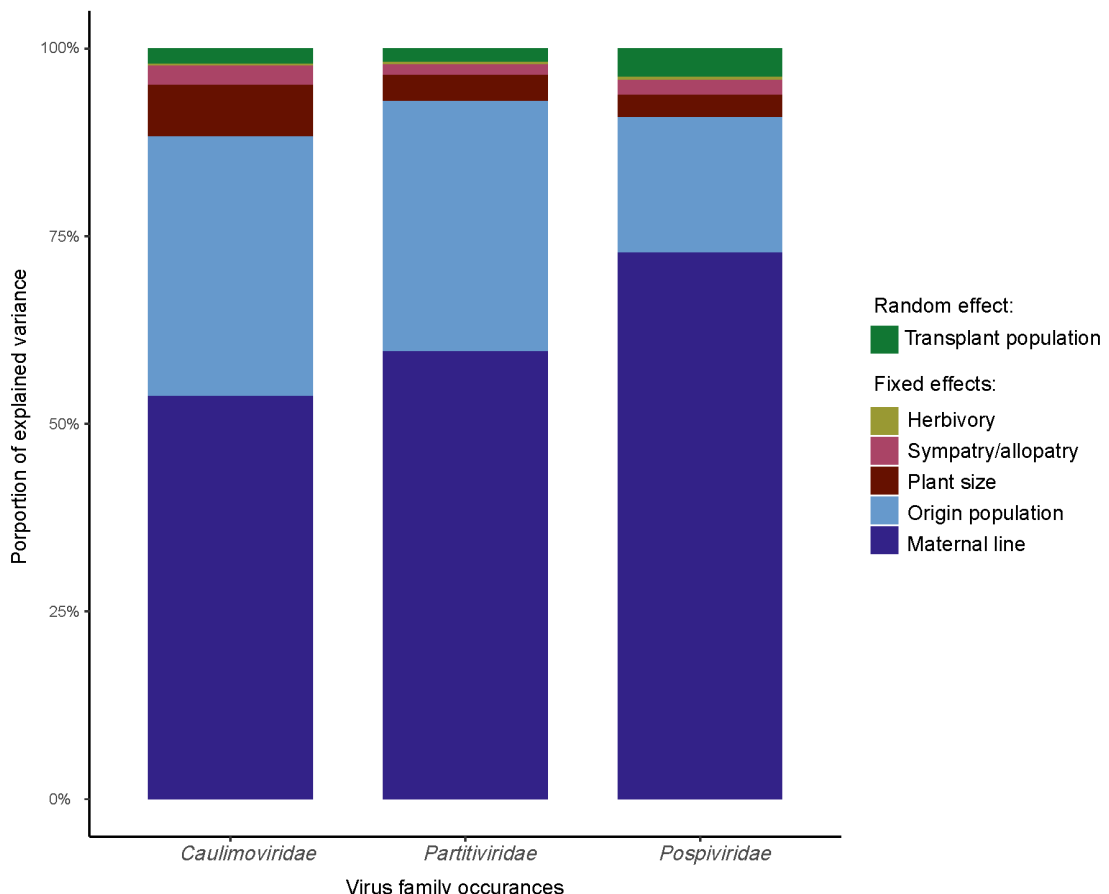
Fixed effect	<i>Wald <math>\chi^2</math></i>	Df	<i>p</i> -value
Plant size	1.71	1	0.190
<b>Seed origin population</b>	<b>9.09</b>	<b>2</b>	<b>0.010</b>
Transplant population	1.64	2	0.438
Seed origin population : sympatry/allopatry	1.53	3	0.673

597

598

599 Figure 3. Variance partitioning of the fixed and random effects in the Hierarchical Modelling  
 600 of Species Communities model for the three most prevalent virus families (*Caulimoviridae*,  
 601 *Partitiviridae*, *Pospiviridae*) in the reciprocal transplant experiment. The six variables  
 602 explaining the occurrences the three virus families were: maternal line, seed origin population,  
 603 plant size, sympatry/allopatry, herbivory and transplant population (random effect).

604



605  
606  
607  
608  
609  
610  
611  
612  
613  
614  
615  
616  
617  
618  
619  
620

621                   **Supplement**

622

623                   **Supplementary table 1.** The host maternal lines included in a reciprocal transplant  
624 experiment studying viral local adaptation in *Plantago lanceolata* host populations in the Åland  
625 Islands during naturally occurring viral epidemics. In the table are included the ID of each  
626 maternal line, the ID of the origin population of each maternal line, the ID of the transplant  
627 population where the plants were placed during the experiment and the number of individuals,  
628 and finally, the number of sequenced individuals.

Maternal line	Seed origin population	Transplant population	No individuals in the experiment	Number of individuals sequenced
876-1	876	876	5	3
876-1	876	950	5	3
876-1	876	9205	5	3
876-2	876	876	5	3
876-2	876	950	5	3
876-2	876	9205	5	3
876-3	876	876	5	3
876-3	876	950	5	3
876-3	876	9205	5	3
876-4	876	876	5	3
876-4	876	950	1	1
876-4	876	9205	0	0
876-5	876	876	5	3
876-5	876	950	4	3
876-5	876	9205	3	3
876-6	876	876	5	3
876-6	876	950	5	3
876-6	876	9205	5	3
876-7	876	876	5	3
876-7	876	950	5	3
876-7	876	9205	5	3
876-9	876	876	5	3
876-9	876	950	5	3
876-9	876	9205	5	3
950-10	950	876	5	3
950-10	950	950	5	3
950-10	950	9205	5	3
950-2	950	876	5	3
950-2	950	950	5	3
950-2	950	9205	5	3
950-4	950	876	5	3
950-4	950	950	5	3
950-4	950	9205	5	3
950-5	950	876	5	3
950-5	950	950	5	3
950-5	950	9205	5	3
950-6	950	876	5	3
950-6	950	950	5	3
950-6	950	9205	5	3
950-7	950	876	5	3
950-7	950	950	5	3
950-7	950	9205	5	3
950-8	950	876	5	3
950-8	950	950	5	3
950-8	950	9205	5	3
950-9	950	876	5	3
950-9	950	950	5	3
950-9	950	9205	5	3

629

630

631

632

633

634

9205-10	9205	876	5	3
9205-10	9205	950	5	3
9205-10	9205	9205	5	3
9205-4	9205	876	5	3
9205-4	9205	950	5	3
9205-4	9205	9205	5	3
9205-5	9205	876	5	3
9205-5	9205	950	5	3
9205-5	9205	9205	5	3
9205-6	9205	876	5	3
9205-6	9205	950	5	3
9205-6	9205	9205	5	3
9205-7	9205	876	5	3
9205-7	9205	950	5	3
9205-7	9205	9205	5	3
9205-8	9205	876	4	3
9205-8	9205	950	5	3
9205-8	9205	9205	5	3
9205-9	9205	876	5	3
9205-9	9205	950	5	3
9205-9	9205	9205	5	3
9250-2	9205	876	5	3
9250-2	9205	950	5	3
9250-2	9205	9205	5	3

---

635

636

637

638

639

640

641

642

643

644 **Supplementary table 2.** Virus families detected by small-RNA sequencing on  
 645 *Plantago lanceolata* individuals (n = 211) included in a transplant experiment in the Åland  
 646 Islands studying viral local adaptation. The genera belonging to each virus family are shown  
 647 as well as the number of contigs and virus species within each virus family. Reference to the  
 648 literature describing the detected family listed in the “reference” column [1–3].

Family	Genus	Contigs	Species	References
<i>Botourmiaviridae</i>		3	1	
	<i>Gammascleroulivirus</i>	3	1	
<i>Caulimoviridae</i>		896	21	[1,2,3]
	<i>Badnavirus</i>	1	1	
	<i>Caulimovirus</i>	842	15	
	<i>Soymovirus</i>	52	5	
<i>Closteroviridae</i>		13	5	[1,2,3]
	<i>Ampelovirus</i>	1	1	
	<i>Closterovirus</i>	11	3	
	unclassified	1	1	
<i>Partitiviridae</i>		212	11	[1,2,3]
	<i>Betapartitivirus</i>	113	8	
	unclassified	99	3	
<i>Pospiviridae</i>		24	1	[3]
	<i>Pospiviroid</i>	24	1	
<i>Tymoviridae</i>		3	1	[1,2,3]
	<i>Maculavirus</i>	3	1	

649

650

651

652

653

654

655

656

657

658           **Supplementary table 3.** Post hoc test comparing the infection status of the host  
 659 *Plantago lanceolata* from the three seed origin populations in a local adaptation experiment in  
 660 the Åland Islands during naturally occurring viral epidemics. Pairwise comparison of the  
 661 estimated marginal means calculated from both generalized linear mixed effects models A)  
 662 model LF and B) model HA (Table 1 and 2). P-values are Tukey adjusted.

**A.**

Contrast	Estimate	SE	Df	Z ratio	p-value
Seed origin population 876 – Seed origin population 950	1.283	0.703	Inf	1.825	0.161
<b>Seed origin population 876- Seed origin population 9205</b>	<b>2.071</b>	<b>0.778</b>	<b>Inf</b>	<b>2.661</b>	<b>0.021</b>
Seed origin population 950 – Seed origin population 9205	0.788	0.736	Inf	1.070	0.532

**B.**

Contrast	Estimate	SE	Df	Z ratio	p-value
Seed origin population 876 – Seed origin population 950	0.703	0.597	Inf	1.176	0.467
<b>Seed origin population 876- Seed origin population 9205</b>	<b>1.818</b>	<b>0.649</b>	<b>Inf</b>	<b>2.802</b>	<b>0.014</b>
Seed origin population 950 – Seed origin population 9205	1.115	0.664	Inf	1.679	0.213

663

664

665

666

667

668

669

670

671

672

673

674

675

676

677

678

679

680

681           **Supplementary table 4.** Model coefficients (model HA) testing for the effects of local

682   adaptation on host infection status using the home *vs.* away metrics of local adaptation. For all

683   variables one levels is a reference level included in the intercept.

684

Parameter	Coefficient	Std. Error	z-ratio	p-value
(Intercept)	0.46958	0.76237	0.61595	0.53792
Plant size	-0.00088	0.00067	-1.31035	0.19008
Seed origin population 950	-1.28293	0.70295	-1.82505	0.06799
<b>Seed origin population 9205</b>	<b>-2.07082</b>	<b>0.77828</b>	<b>-2.66078</b>	<b>0.00780</b>
Transplant population 950	-0.47045	0.67071	-0.70142	0.48304
Transplant population 9205	0.28314	0.59902	0.47267	0.63645
Seed origin population 876 × sympatric	-0.86730	0.80862	-1.07257	0.28346
Seed origin population 950 × sympatric	0.29316	0.83422	0.35141	0.72528
Seed origin population 9205 × sympatric	-0.36200	0.92003	-0.39346	0.69398

685

686

687       Supplementary table 5. Explanatory and predictive performance of the HMSC model  
 688       of viral occurrence in the experimental plant individuals in terms of Tjur  $R^2$  and AUC. The  
 689       model predictive performance is based on 10-fold cross-validation.

690

Response variable	Model explanatory performance		Model predictive performance with 10-fold cross validation (cv)	
	Tjur $R^2$	AUC	Tjur $R^2$ (cv)	AUC (cv)
<i>Caulimoviridae</i>	0.24	0.91	0.16	0.81
<i>Partitiviridae</i>	0.47	0.98	0.4	0.88
<i>Pospivirodae</i>	0.1	0.8	0.01	0.54

691

692

693

694           **Supplementary table 6.** Exact values of the HMSC model variance partitioning for the  
695           three most prevalent virus families detected in a reciprocal transplant experiment studying local  
696           adaptation. Six variables explaining the virus family occurrence in a reciprocal transplant  
697           experiment were: maternal line ID, seed origin population ID, sympatry/allopatry, plant size,  
698           herbivory and transplant population ID (random).

699

---

Model parameter	Response variable		
Fixed effects:	<i>Caulimoviridae</i>	<i>Partitiviridae</i>	<i>Pospivirodae</i>
Maternal line	0.54	0.60	0.73
Seed origin population	0.35	0.33	0.18
Sympatry/allopatry	0.03	0.02	0.02
Plant area	0.07	0.03	0.03
Herbivory	0	0	0
Random effect:			
Transplant population	0.02	0.02	0.04

700  
701  
702  
703  
704  
705

706 **References**

707

708 1. Hammond J. 1982 Plantago as a host of economically important viruses. *Adv. Virus Res.*  
709 **27**, 103–140. (doi:10.1016/S0065-3527(08)60434-0)

710 2. Susi H, Filloux D, Frilander MJ, Roumagnac P, Laine AL. 2019 Diverse and variable  
711 virus communities in wild plant populations revealed by metagenomic tools. *PeerJ*  
712 **2019**. (doi:10.7717/peerj.6140)

713 3. Norberg A, Susi H, Sallinen S, Baran P, Clark NJ, Laine AL. 2023 Direct and indirect  
714 viral associations predict coexistence in wild plant virus communities. *Curr. Biol.* **33**,  
715 1665-1676.e4. (doi:10.1016/J.CUB.2023.03.022)

716

717